Noise Performance of Negative-Resistance Compensated Microwave Bandpass Filters—Theory and Experiments

Kwok-Keung M. Cheng, *Member, IEEE,* and Hil-Yee Chan

***Abstract*—This paper examines both theoretically and experimentally the dependency of in-band noise performance upon circuit and device parameters of microwave filters employing negative-resistance compensation. By neglecting the influence of the induced gate noise source, a general expression for evaluating the noise figure of a second-order active filter is derived as a function of design parameters such as the transistor's noise figure, inductor's quality factor, and filter's bandwidth. In addition, factors affecting the optimization of the overall noise figure of these filters are discussed. For verification, the measured performance of two 900-MHz experimental MESFET filters are included.**

***Index Terms*—Microwave active filters, negative-resistance, noise figure.**

I. Introduction

FOR FULLY integrated microwave transceivers, there is considerable interest in filter design for monolithic-microwave integrated-circuit (MMIC) realization. Unfortunately, at microwave frequencies, the Q factor of the on-chip inductors is typically low and, hence, passive MMIC filters usually exhibit high-insertion loss and poor selectivity. In recent years, the negative-resistance techniques [1], [2] have been proposed for use in MMIC filters to compensate for component losses, especially of the spiral inductors. These techniques enable the design of microwave active filters with zero insertion loss and excellent channel selectivity. While active filters have the major advantages of small size with high selectivity, their limitations in terms of the power handling and noise figure have not received close attention. In fact, only a few reports have been published [3], [4] on the study of noise performance of microwave active filters. In this paper, the in-band noise behavior of a second-order bandpass filter employing negative resistance compensation is investigated. Analytical expressions are derived to relate the overall noise figure of the filter to various circuit and device parameters such as the transistor's noise figure, inductor's Q factor, filter's bandwidth, etc. These equations also provide a good understanding of the fundamental limitations in attaining low noise-figure values in microwave active filters. Finally, the measured and predicted noise performances of two experimental filter circuits operating at 900 MHz are shown for comparison.

Manuscript received September 15, 2000.

The authors are with the Department of Electronic Engineering, The Chinese University of Hong Kong, Shatin, Hong Kong.

Publisher Item Identifier S 0018-9480(01)03322-1.

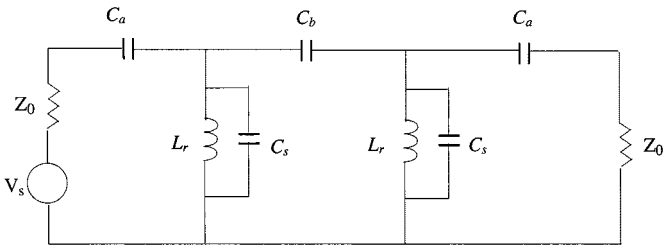

Fig. 1. Lossless lumped-element bandpass filter.

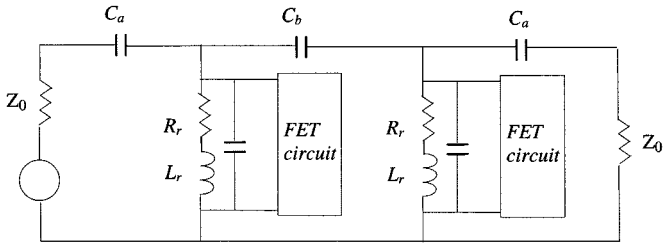

Fig. 2. Lossy filter with negative-resistance compensation.

II. Active Filters Employing Negative-Resistance Circuits

Among the many active filter topologies, the direct coupling of negative-resistance circuits to a coupled-resonator (*LC*) filter [1], [2] has been widely studied due to its simplicity in structure. Without loss of generality, the lumped-element second-order bandpass filter topology [5], shown in Fig. 1, is used in the analyses (for design equations, see the Appendix). Such a configuration is well-suited for MMIC implementation because it does not require large distributed elements. Fig. 2 shows how negative-resistance circuits may be employed to compensate for the inductor losses. The negative-resistance circuit (Fig. 3) basically comprises a MESFET, a feedback capacitor C_f, and an external gate-to-source capacitor C_{ext}. Note that the value of R_{neg} is frequency dependent and, thus, this technique is usable only for narrow-band applications. Under the assumption that $Q \gg 1$, where $Q = \omega_0 L_r / R_r$, the condition for exact cancellation of the inductor loss by the negative-resistance circuit has been shown elsewhere [6] as

$$R_{\text{neg}} = \frac{1}{g_0} = Q^2 R_r. \tag{1}$$

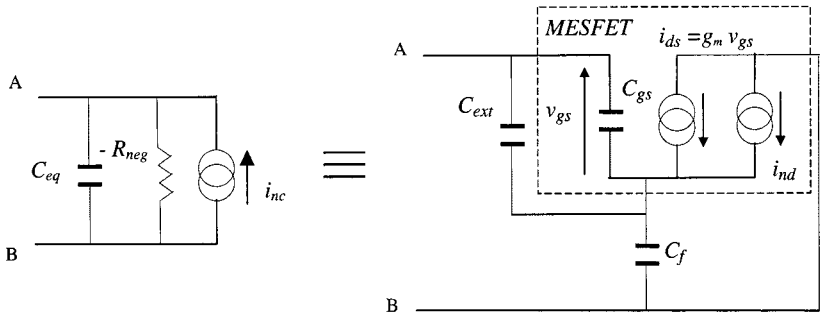

Fig. 3. Noise model of the negative-resistance circuit.

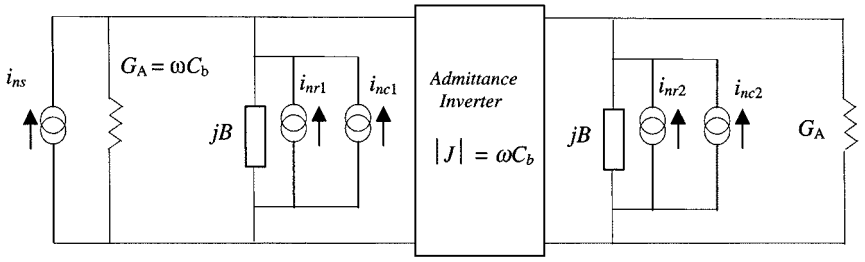

Fig. 4. Noise analysis: filter circuit model.

Subsequently, the value of C_f may be evaluated by the following equation:

$$\frac{C_{f(\pm)}}{C_T} = \frac{\alpha}{2} - 1 \pm \sqrt{\alpha\left(\frac{\alpha}{4} - 1\right) - \frac{\alpha^2}{\beta^2}} \tag{2}$$

where

$$\alpha = \frac{g_m}{g_0}$$
$$\beta = \frac{\omega_0 C_T}{g_0}$$
$$C_T = C_{gs} + C_{\text{ext}}.$$

It can be seen that there are two possible solutions for C_f, labeled by $C_{f(+)}$ and $C_{f(-)}$, provided that

$$g_m > 4g_0 \tag{3}$$

and

$$C_T > \frac{2g_0}{\omega_0\sqrt{1 - \frac{4}{\alpha}}}. \tag{4}$$

III. Noise Analysis

In order to perform the noise analysis of the active filter, the MESFET is assumed to be modeled by the equivalent circuit shown in Fig. 3, in which the drain noise current (i_{nd}) is the only noise source being considered here. Note that the induced gate noise current is ignored due to its relatively small value at a low gigahertz frequency range. As a result, the expression for the 50-Ω (i.e., unmatched) noise figure of the FET can be written as

$$F_{50} = 1 + \frac{|i_{\text{nd}}|^2}{4kT\Delta f}\,\frac{1 + \omega^2 C_{gs}^2 Z_0^2}{Z_0 g_m^2} \tag{5}$$

where k is the Boltzmann's constant, $T = 290$ K, and Δf is the bandwidth of the measuring system. Given that $\omega C_{gs} Z_0 \ll 1$, the inherent noise power generated by the device may, therefore, be determined by the following equation:

$$\frac{|i_{\text{nd}}|^2}{4kT\Delta f} \approx (F_{50} - 1)\, Z_0 g_m^2. \tag{6}$$

In addition, the relationship between the short-circuit noise current (i_{nc}) of the negative-resistance circuit (Fig. 3) and the internal noise current of the FET (i_{nd}) can be formulated as

$$|i_{\text{nc}}|^2 = \frac{|i_{\text{nd}}|^2}{\left(1 + \frac{C_f}{C_T}\right)^2 + \left(\frac{g_m}{\omega C_T}\right)^2} = \frac{|i_{\text{nd}}|^2}{\alpha\frac{C_f}{C_T}}. \tag{7}$$

For the narrow-band filter under consideration, the equivalent circuit shown in Fig. 4 may thus be used for evaluating the overall in-band noise behavior of the filter, including both the noise contributions from the loss resistances of the inductors, as well as the current noise generated by the FETs. Based upon the linear circuit theory, the overall noise figure and insertion loss of the compensated filter, at any spot frequency (ω) within the 3 –dB bandwidth (BW), can, therefore, be derived as

$$F = 1 + \frac{|i_{nr1}|^2 + |i_{nc1}|^2}{|i_{ns}|^2} + \frac{|i_{nr2}|^2 + |i_{nc2}|^2}{|i_{ns}|^2}\left(1 + \frac{B^2}{\omega_0^2 \mathrm{C}_{\mathrm{b}}^2}\right) \tag{8}$$

$$|S_{21}|^2 = \frac{1}{1 + \frac{B^4}{4\omega_0^4 \mathrm{C}_{\mathrm{b}}^4}} \tag{9}$$

where

$$B = 2C_r(\omega - \omega_0)$$
$$|i_{ns}|^2 = 4kT\Delta f \omega_0 \mathrm{C}_{\mathrm{b}}$$
$$|i_{nr1}|^2 = |i_{nr2}|^2 = 4kT\Delta f g_0$$
$$|i_{nc1}|^2 = |i_{nc2}|^2 = |i_{\text{nc}}|^2.$$

B is the effective shunt susceptance of the resonant circuits. Furthermore, with reference to the Appendix, we have

$$\left(\frac{B}{\omega_0 \mathrm{C_b}}\right)^2 = \left(2C_r \frac{\omega-\omega_0}{\omega_0 C_b}\right)^2 = 2\left(2\frac{\omega-\omega_0}{\mathrm{BW}}\right)^2. \quad (10)$$

Combining (8) and (10), we obtain

$$F = 1 + \left\{\frac{g_0}{\omega_0 \mathrm{C_b}} + \frac{|i_{\mathrm{nc}}|^2}{4kT\Delta f \omega_0 \mathrm{C_b}}\right\}\left\{2 + 2\left(2\frac{\omega-\omega_0}{\mathrm{BW}}\right)^2\right\}. \quad (11)$$

Finally, by substituting (6) and (7) into (11), the in-band noise figure of the filter may be expressed as follows:

$$F = 1 + K\left\{1 + \left(2\frac{\omega-\omega_0}{\mathrm{BW}}\right)^2\right\}$$

where

$$K = \frac{2\sqrt{2}}{\mathrm{Q}}\left(\frac{\omega_0}{\mathrm{BW}}\right)\left\{1 + g_m Z_0 \frac{F_{50}-1}{C_f/C_T}\right\}. \quad (12)$$

The above expression reveals the influence of circuit and device parameters on the overall noise performance of the filter circuit.

1) The value of C_f/C_T has a direct effect on the noise figure, especially when the FET is the dominant noise source. This formula suggested that a large value of C_f should be chosen [i.e., $C_{f(+)}$] for the improved noise performance.
2) Losses within the passive part of the filter, characterized by the inductor Q factor, have a strong effect on the overall noise behavior. Equation (12) indicated that the noise figure decreases with increasing Q value.
3) The overall noise figure of the filter is a direct function of the center frequency-to-bandwidth ratio (ω_0/BW).
4) Minimum noise figure occurs at midband and it increases with increasing offset frequency within the 3-dB bandwidth.
5) If the noise contribution from the active device is assumed to be negligibly small, the theoretical noise figure of the filter can be stated as

$$F = 1 + \frac{2\sqrt{2}}{\mathrm{Q}}\left(\frac{\omega_0}{\mathrm{BW}}\right). \quad (13)$$

IV. Experiments and Discussions

In order to verify the validity of the above theory, noise-figure measurements were performed on experimental filters constructed using lumped components. The negative-resistance circuits employed here consist of a Siemens CFY 30 GaAs MESFET ($F_{50} = 3$ dB) with chip capacitors ($C_{\mathrm{ext}} = 2$ pF) connected between the gate and source terminals. In the absence of the FET circuits, the passive design was found to have an insertion loss of about 10 dB, with a center frequency of around 900 MHz. Using the design equation given in the Appendix, the value of $g_0$was estimated to be approximately 2.8 mS ($L_r = 2.5$ nH, $R_r = 0.6\ \Omega$, $Q = 25$).

Fig. 5 shows the measured small-signal frequency responses of the two fabricated filter circuits, with almost zero insertion loss at midband, at a device drain current I_{ds} of 12 mA, and

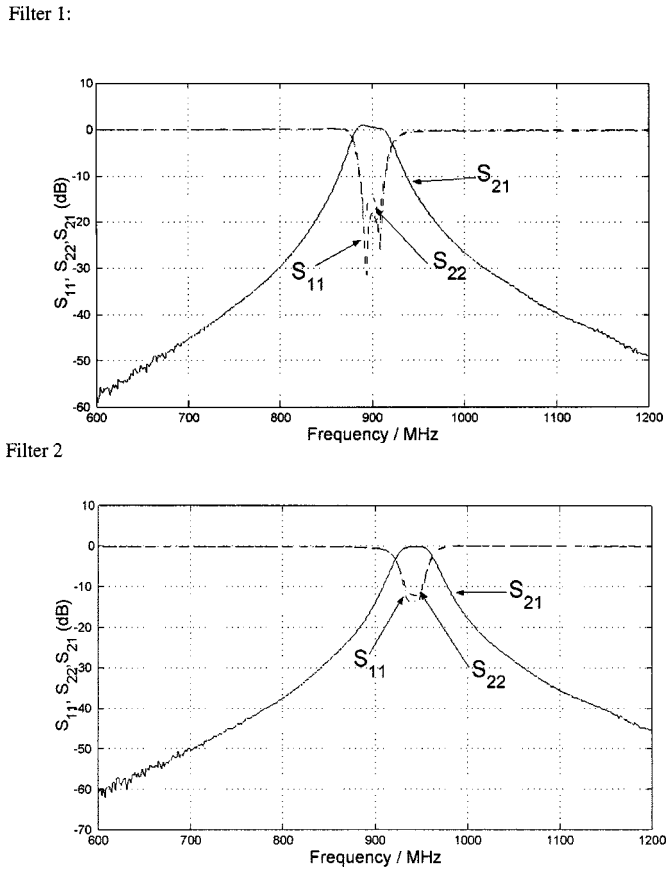

Fig. 5. Measured frequency responses of the experimental active filters.

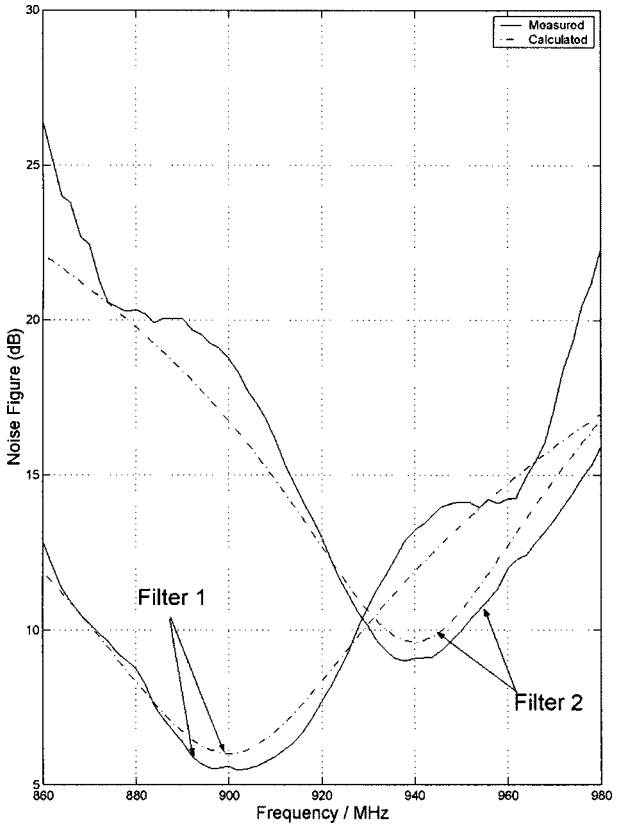

Fig. 6. Predicted and measured noise-figure curves versus frequency.

TABLE I
COMPARISON OF CALCULATED AND MEASURED NOISE-FIGURE VALUES

	C_f/C_T	Center Frequency	Bandwidth	Calculated Noise Figure (mid-band)	Measured Noise Figure (mid-band)
Filter 1	7.2	900 MHz	41 MHz	6.0 dB	5.6 dB
Filter 2	0.83	940 MHz	37 MHz	9.6 dB	9.1 dB

$g_m \approx 30$ mS (hence, $\alpha \approx 10$). In the experiments, noise-figure measurements were conducted for both circuits and the results are plotted in Fig. 6 for illustrative purposes. For comparative purposes, both the predicted and measured midband noise-figure values of the filters are tabulated in Table I. It can be seen from this table that the discrepancies between the calculated and experimental data are small (less than 0.5 dB). In addition, the variations of the noise figures within the 3-dB bandwidth is in good agreement with the derived expression.

V. CONCLUSIONS

A systematic study of the in-band noise behavior of negative-resistance compensated bandpass filters has been presented in this paper. A general analytical expression governing the overall noise figure of the filter as a function of circuit and device parameters has been developed. This formula suggested that further improvement of noise performance may be achieved by compromising linearity [6]. Good agreement is observed between the predicted and measured noise-figure values for both experimental filters. Finally, the method of analysis described here can easily be extended to higher order active filter design.

APPENDIX

Here, we provide the design equations for the Butterworth bandpass filter shown in Fig. 1. Under the narrow-band assumption, the component values can be evaluated by the following expressions [5]:

$$\omega_0 C_r = \frac{1}{\omega_0 L_r} \tag{A1}$$

$$\omega_0 C_b = \frac{1}{\sqrt{2}\omega_0 L_r}\left(\frac{\mathrm{BW}}{\omega_0}\right) \tag{A2}$$

$$\omega_0 C_a Z_0 = \sqrt{\frac{\omega_0 C_b Z_0}{1-\omega_0 C_b Z_0}} \tag{A3}$$

$$C_s = C_r - C_b - C_a + \omega_0 C_b Z_0 C_a \tag{A4}$$

$$\mathrm{BW} = \omega_u - \omega_L \tag{A5}$$

where ω_L, ω_U, and ω_0 are the lower cutoff, upper cutoff, and center frequencies (in radians per second) of the passband characteristics, respectively. Furthermore, , the insertion loss of the filter may be calculated by

$$\left.\frac{1}{S_{21}}\right|_{\omega=\omega_0} = \frac{1+\left(1+\dfrac{\sqrt{2}}{Q}\dfrac{\omega_0}{\mathrm{BW}}\right)^2}{2}. \tag{A6}$$

REFERENCES

[1] U. Karacaoglu and I. D. Robertson, "MMIC active bandpass filters using varactor-tuned negative resistance elements," *IEEE Trans. Microwave Theory Tech.*, vol. 43, pp. 2926–2932, Dec. 1995.

[2] V. Aparin and P. Katzin, "Active GaAs MMIC bandpass filters with automatic frequency tuning and insertion loss control," *IEEE J. Solid-State Circuits*, vol. 30, pp. 1068–1073, Oct. 1995.

[3] E. C. Krantz and G. R. Branner, "Active microwave filters with noise performance considerations," *IEEE Trans. Microwave Theory Tech.*, vol. 42, pp. 1368–1378, July 1994.

[4] H. Ezzedine, L. Billonnet, B. Jarry, and P. Guillon, "Optimization of noise performance for various topologies of planar microwave active filters using noise wave techniques," *IEEE Trans. Microwave Theory Tech.*, vol. 46, pp. 2484–2492, Dec. 1998.

[5] G. L. Matthaei, L. Young, and E. M. T. Jones, *Microwave Filter Impedance Matching Networks and Coupling Structures*. New York: McGraw-Hill, 1964.

[6] K. K. M. Cheng and S. C. Chan, "Reduction of intermodulation distortion in microwave active bandpass filters: Theory and experiments," *IEEE Trans. Microwave Theory Tech.*, vol. 48, pp. 221–225, Feb. 2000.

Kwok-Keung M. Cheng (S'90–M'91) received the B.Sc. degree (with first-class honors) in electrical engineering and the Ph.D. degree from King's College, University of London, London, U.K., in 1987 and 1993, respectively.

From 1990 to 1992, he was a Research Assistant at King's College, where he was involved in the area of hybrid circuit and MMIC design, and from 1993 to 1995, he was a Post-Doctoral Research Associate, involved in the investigation of coplanar structures for microwave/millimeter-wave application. In 1996, he became an Assistant Professor in the Department of Electronic Engineering, The Chinese University of Hong Kong, Hong Kong. He has authored or co-authored over 35 papers published in leading international journals and conferences, and was a contributing author of *MMIC Design* (London, U.K.: IEE Press, 1995). His current research interests are concerned with the design of MMICs, oscillators, active filters, and power amplifiers.

Dr. Cheng was the recipient of the 1986 Siemens Prize, the 1987 Institution of Electrical Engineers (IEE) Prize, and the 1988 Convocation Susquicentennial Prize in Engineering (University of London).

Hil-Yee Chan received the B.Eng. and M.Phil. degrees in electronic engineering from The Chinese University of Hong Kong, Hong Kong, in 1998 and 2000, respectively.

His current research interests are in the areas of filter design and wireless communications.